Current status of the "Hybrid Kurotama model" for total reaction cross sections

L. Sihver[1*], A. Kohama[2], K. Iida[3], K. Oyamatsu[4], S. Hashimoto[5], H. Iwase[6], and K. Niita[7]

[1]Chalmers University of Technology, Nuclear Engineering, Applied Physics, SE-412 96 Göteborg, Sweden
[2]RIKEN, Nishina Center, RIKEN, 2-1, Hirosawa, Wako-shi, Saitama 351-0198, Japan
[3]Kochi University, Department of Natural Science, Faculty of Science, 2-5-1 Akebono-cho, Kochi 780-8520, Japan
[4]Aichi Shukutoku University, Department of Human Informatics, 2-9 Katahira, Nagakute, Aichi, 480-1197, Japan
[5]Japan Atomic Energy Agency, Shirakata-Shirane 2-4, Tokai, Ibaraki, 319-1195, Japan
[6]High Energy Accelerator Research Organization, Oho 1-1, Tsukuba, Ibaraki, 305-0801, Japan
[7]Research Organization for Information Science and Technology, Shirakata-Shirane 2-4, Tokai, Ibaraki, 319-1106, Japan

Abstract

To be able to calculate the nucleon+nucleus and nucleus+nucleus total reaction cross sections with precision is of great importance for studies of fundamental nuclear properties, e.g., the nuclear structure. This is also very important for particle and heavy ion transport calculations since in all particle and heavy ion transport codes, the probability function according to which a projectile particle will collide within a certain distance in a matter depends on the total reaction cross sections. This will also scale the calculated partial fragmentation cross sections. It is therefore crucial that accurate total reaction cross section models are used in the transport calculations. In this paper, a new general purpose total reaction cross section model/subroutine called "Hybrid Kurotama" is presented. The model has been tested against available p+He, p+nucleus, and nucleus+nucleus total reaction cross sections and an overall better agreement has been found than for earlier published models. This model is therefore very suitable to be used in any deterministic or Monte Carlo particle and heavy ion transport code.

[*]Corresponding author.
Phone:+46-31-772 2921
Fax:+46-31 772 3079
E-mail: sihver@chalmers.se

submitted to *Nucl. Inst. Meth. B*

1. Introduction

The total reaction cross section, σ_R, of a nuclear reaction is a fundamental observable that characterizes the geometrical size of the nuclei. Accurate knowledge of the nucleon+nucleus and nucleus+nucleus σ_R is therefore of great importance for our understanding of the fundamental nuclear properties, e.g., the nuclear structure. Particle and heavy ion transport includes many complex processes, while measurements for all possible systems, ranging from biological effects to critical organs to people exposed to ionizing radiation, would be impractical or too expensive; e.g. direct measurements of dose equivalents to organs in humans cannot be performed for understandable reasons. A reliable and accurate particle and heavy ion transport code is therefore an essential tool when designing accelerator facilities as well as for many other various applications. The σ_R and the decay lifetime of a projectile particle are essential quantities when determining the mean free path of a transported particle since in all particle and heavy ion transport codes, the probability function according to which a projectile particle will collide within a certain distance in the matter depends on the σ_R. This will also scale the calculated partial fragmentation cross sections.

During the last decades many new applications have also arisen within transmutation and reactor science, space and nuclear medicine, radiotherapy in particular, and many accelerator facilities are operating or planned for construction. There is therefore a need to improve and benchmark the available particle and heavy ion transport codes. To be able to calculate complex geometries, including production and transport of protons, neutrons, and α particles, 3-dimensional (3D) transport using Monte-Carlo (MC) technique must be used. Radiation protection studies for crews of international flights at high altitude have also received considerable attention in recent years and to be able to perform correct estimations of organ and effective doses, MC simulations are needed. In all MC particle and heavy ion transport codes, the next collision point is simulated using the MC method and the calculated σ_R.

Due to calculation speed, simplicity and accuracy, semi-empirical parameterization models for the total reaction cross section are most often used in these codes. The aim of this paper, is to present a new general purpose total reaction cross section model/subroutine called “Hybrid Kurotama”, which is based on the Black Sphere (“kurotama" in Japanese) cross section formula [1] with its extension to low energies by smoothly connecting it to the semi-empirical cross section parameterization developed by Tripathi et al. [2,3,4].

2. Model description

In order to systematically estimate σ_R for nucleus+nucleus reactions, we apply the Black Sphere (BS) cross section formula [1]. It was originally constructed for σ_R of proton-nucleus reactions in the framework of the BS approximation of nuclei, in which a nucleus is viewed as a BS with the radius “a” [5]. A reference BS radius “a_0” was set to the BS radius at E_P = 800 MeV and Δa is the deviation of a from a_0 at given E_p above 100 MeV, as described in ref. [5]. “a_0” is

determined by fitting the angle of the first elastic diffraction peak calculated for proton diffraction by a circular black disk of radius "a_0" to the measured value. For systematic estimation of σ_R, we adopt the mass number dependence as a_0=1.2671 $A^{1/3}$ -0.152 fm for $A \geqq 50$ and a_0=1.2671 $A^{1/3}$ -0.152 fm for A<50 [6]. The σ_R is then calculated according to:

$$\sigma_R = \pi a^2{}_0 \, (1 + \frac{\Delta a}{a_0})^2 \qquad (1)$$

This assumes the incident protons are point particles leading to vanishing cross section for the proton-proton case. In this formula, the geometrical cross section, πa^2, is expressed as a function of the mass and neutron excess of the target nucleus and of the proton incident energy, E_p, in a way free from any adjustable E_p dependent parameter. The dependence of σ_R on E_p has been deduced from a simple argument involving the nuclear "optical" depth for incident protons [1]. This formula can easily be extended to nucleus+nucleus reactions by using $\pi(a_P + a_T)^2$, where a_P (a_T) denotes the BS radius of a projectile (target) [1,6,7,8] and it can reproduce the empirical data remarkably well above 100 MeV/nucleon [1,6,7,8]. Note that no Coulomb effect is yet included. For some specific reactions, a_0 is set to be a value determined from the measured angle of the first diffraction maximum in proton elastic scattering [5,8], which may slightly fluctuate around the mass number dependence described above.

3. Subroutine Hybrid Kurotama in PHITS

The BS model assumes that the target nucleus is strongly absorptive to the incident particle and can therefore be considered as a BS. The BS radius, a, is evaluated from measured elastic diffraction peaks and then identified as a typical length scale characterizing the nuclear size. In the subroutine "Kurotama", the BS radius is set automatically based on a function, and as fixed values for special cases. However, the BS model requires that the de Broglie wavelength of the proton is considerably smaller than the nuclear size and the BS model therefore breaks down below around 100 MeV/u. In addition to that, the Coulomb repulsion causes resonance features and a sharp increase of σ_R at energies below 100 MeV/nucleon, at which an energy dependent transparency parameter and the influence of the Fermi motion and Coulomb effects should be included. To solve the limitations of the BS model at low energies and to create a general purpose total reaction cross section model which can also be used for reactions with projectile energies below around 100 MeV/nucleon, the BS model has been connected to the parameterization developed by Tripathi et al. [2,3,4], which has been shown to be one of the best available total reaction cross section systematics [10,11,12], at E_{cut} = 115 MeV/nucleon. In order to smoothly connect the two curves (Kurotama and Tripathi) at the projectile energy $E_{cut,}$, a two parameter Fermi function, $f_{cut1(2)}$ (E_P), was adopted according to:

$$\sigma_R\,(E_P) = f_{cut1}\,(E_P) * \pi\,(a_P(E_P) + a_T(E_P))^2 + f_{cut2}\,(E_P) * \sigma_{Trip}(E_P) * \pi(a_P(E_{cut}) + a_T(E_{cut}))^2/\sigma_{Trip}(E_{cut}) \qquad (2)$$

where:

$a_P(E_P)$ is the black sphere radius of the projectile at the projectile energy E_P
$a_T(E_P)$ is the black sphere radius of the target at the projectile energy E_P
$\sigma_{Trip}(E_P)$ is the total reaction cross section according to the parameterization by Tripathi et al. [2,3,4].
E_{cut}= 115 MeV/nucleon, d = 1 MeV/nucleon.
$f_{cut1}(E_P) = 1/(1+\exp((E_p-E_{cut})/d))$,
$f_{cut2}(E_P) = 1/(1+\exp((-E_p + E_{cut})/d))$.

This hydrid model is called "Hybrid Kurotama". It is to be noted that the absolute values of Tripathi's formula are renormalized in such a way as to agree with the value of Hybrid Kurotama at E_{cut},. as described above. Due to its ability to reproduce the total reaction cross sections for nucleus+nucleus reaction over a wide energy range, the Hybrid Kurotama model has been officially incorporated into PHITS [9] from version 2.52. In Figure 1, a comparison of the calculated total reaction cross sections for $^{12}C+^{12}C$ using the original BS model, the Hybrid Kurotama model, and the Tripathi parameterization are shown together with experimental data refs [13-18]. In Figure 1, it can be seen that the first version of the "Hybrid Kurotama" can very precisely reproduce the empirical energy dependence of σ_R over a wide energy region. In particular, they are consistent with the latest experimental data [13]. However, this version of the Hybrid Kurotama is not able to handle complex targets consisting of several different nuclei, or targets with components of natural abundances. There is also a limitation in the energy of the projectile set to 5 GeV/nucleon above which cross sections are not able to be calculated. There is also a significant over estimation of the cross section at low energies for p+He and He+nucleus reactions, as can be seen in Figures 2 and 3, where calculated results are shown together with data from refs. [18-44]. The Hybrid Kurotama model has therefore been improved, and the improved version will be discussed in the next section.

4. Improvements of the Kurotama subroutine

A new and improved version of the Hybrid Kurotama model/subroutine, which can handle complex targets containing different target nuclei, as well as target nuclei with natural abundances, for projectile energies well above 10 GeV/nucleon has now been developed. The energy dependence of the Hybrid Kurotama model is only driven by that of the nucleon-nucleon total cross sections, the parameterization of which is followed by ref. [45] up to 5 GeV/nucleon. Above 5 GeV/nucleon, we assume that the nucleon-nucleon total cross sections are energy independent and equal to those at 5 GeV/nucleon. The uncertainty due to this approximation will stay in a few % up to around 100 GeV/nucleon [46]. The fact that the total reaction cross sections for proton + nucleus reactions stays roughly constant at energies above 5-10 GeV/nucleon, and for nucleus+ nucleus reactions above some GeV/nucleon, was studied and

confirmed during the 80^{ths} and 90^{ths}, when the concept of limiting fragmentation was carefully experimentally confirmed [47-50].

The behavior of the cross sections at energies below around 350-450 MeV/nucleon is quite different for p+He and He+nucleus reactions than for p+nucleus and nucleus+nucleus reactions. To create a general total reaction cross section model, which can also simulate the experimental results for all p+He/He+p, He+nucleus/nucleus reactions, E_{cut} = 400 MeV/nucleon has been chosen for these reactions, in addition to the E_{cut} = 115 MeV/nucleon for all other reactions. In order to smoothly connect the Kurotama with the parameterization performed by Tripathi et al. [2,3,4] at E_{cut} = 400 MeV/nuclon, a two parameter Fermi function was used in the same way as shown in Eq. (2). This improved Hybrid Kurotama model has been benchmarked against available experimental total reaction cross section data, and some examples are shown in Figures 4-14. One can see the improvement due to the introduction of E_{cut} = 400 MeV/nucleon by comparing Fig. 4 with Fig. 2 and Fig. 9 with Fig. 3. As can be seen from these figures, the calculated results for the improved Hybrid Kurotama model/subroutine show an overall better agreement with the experimental data than the results for the model developed by Tripathi et al. The Hybrid Kurotama model is therefore a very suitable model to be used as a subroutine in any deterministic or Monte Carlo particle and heavy ion transport code.

5 Results/conclusion

In this paper, a new general purpose total reaction cross section model/subroutine called "Hybrid Kurotama" is presented. Comparisons of calculated total reaction cross sections for p+He, p+nucleus, and nucleus+nucleus reactions is presented against the results from the parameterization developed by Tripathi et al. [2,3,4] and available measured total reaction cross sections. As can be seen from the results of this study, an overall better agreement between the calculated results for the Hybrid Kurotama model and the measured cross sections is found than between the results from parameterization developed by Tripathi et al. [2,3,4] and the experimental data. Since the model developed by Tripathi et al. is regarded as one of the best available semi-empirical total reaction cross section models, we conclude that the Hybrid Kurotama model/subroutine is currently the best available model. The Hybrid Kurotama model is therefore very suitable to be used as a subroutine in any deterministic or Monte Carlo particle and heavy ion transport code. In particular, the Hybrid Kurotama model is suitable for simulations related to radiation protection, dosimetry, reactor science, space and nuclear medicine, particle therapy in particular, because the data reproducibility for the energy regions of interest for these applications is very good compared to any other previously published models.

Future possible improvements of the Kurotma model include adding the effects of Coulomb dissociation, which is relevant for reactions between heavy nuclei [96], as well as the Coulomb effects, Fermi motion and transparency at low energies to remove the connection to the parameterization developed by Tripathi et al.

Acknowledgements

This study is supported by RIKEN iTHES project. L. Sihver greatly acknowledges A. Kohama for his kind help and support during Sihver's two months stay at RIKEN, Japan. The authors also acknowledge M. Lantz for helping find some of the experimental data used in this study.

References

[1] K. Iida, A. Kohama, and K. Oyamatsu, J. Phys. Soc. Japan **76** (2007) 044201.
[2] R.K. Tripathi, F.A. Cucinotta and J.W. Wilson, 151 Nucl. Instr. Meth. **B 117** (1996) 347-349.
[3] R.K. Tripathi, J.W. Wilson and F.A. Cucinotta, Nucl. Instr. Meth. **B 129** (1997) 11-15.
[4] R.K. Tripathi, F.A. Cucinotta and J. W. Wilson, Nucl. Instr. Meth. **B 155** (1999) 349-356.
[5] A. Kohama, K Iida, and K. Oyamatsu, Phys. Rev. C **69** (2004) 064316.
[6] A. Kohama, K. Iida and K. Oyamatsu, unpublished.
[7] A. Kohama, K. Iida, and K. Oyamatsu, Phys. Rev. C **78** (2008) 061601.
[8] A. Kohama, K Iida, and K. Oyamatsu, Phys. Rev. C **72** (2005) 024602.
[9] T. Sato et al., J. Nucl. Sci. Technol. **50:9** (2013) 913-923.
[10] L. Sihver, M. Lantz, M. Takechi, A. Ferrari, F. Cerutti and T. Sato, IEEEAC paper 1476, ISBN/ISSN: 978-142443888-4 (2010).
[11] L. Sihver, M. Lantz, M. Takechi, A. Kohama, A. Ferrari, F. Cerutti and T. Sato, Adv. Space Res. **49**, 812-819 (2011), doi:10.1016/j.asr.2011.11.029.
[12] L. Sihver, M. Lantz, T.T. Böhlen, A. Mairani, A.F. Cerutti and A. Ferrari, IEEEAC paper 1306, ISSN:1095-323X (2012).
[13] M. Takechi et al., Phys. Rev. C **79** (2009) 061601.
[14] S. Kox et al., Nucl. Phys. **A 420**, 162-172 (1984).
[15] S. Kox et al., Phys. Rev. C **35** (5) 1678-1691 (1987).
[16] Y. Hostachy et al., Nuclear Physics A, Vol. **490**, 441-470 (1988).
[17] C Perrin et al., Phys. Rev. Lett. **49,** 1905-1909 (1982).
[18] J. Jaros, Phys. Rev. C **18,** 2273-2292 (1978).
[19] A.M. Sourkes, A. Houdayer, W.T.H. van Oers, R.F. Carlson and R.E. Brown, Phys. Rev. C **13** (1976) 451-460.
[20] D.E.Velkley, J.D. Brandenverger, D.W. Glascow, T McElistrem, J.C. Manthuruthil, and C.P. Poirier, Phys. Rev. C **7** (1973) 1736.
[21] L. Riidford and A.W. Wlissiona, Proc. Royal Soc. (London) A **257** (1960) 316.
[22] G.N. Velichko, A.A. Vorob'ev, Yu.K. Zalite, G.A. Korolev, E.M. Maev, N.K. Terent'ev, Y. Terrien and A.V. Khanzadeev, Yad. Fiz. **35** (1982) 270 and Sov. J. Nucl. Phys. **35** (1982) 154.
[23] V. Kozoda et al., Sov. Phys. JETP **11** (1960) 511.

[24] G.J. Igo, J.L. Friedes, H. Palevsky, R. Sutter, G. Bennet, W.D. Simpson, D.M. Corley and R.L. Stearns, Nucl. Phys. B **3** (1967) 181.
[25] D.J. Cairns, T.C. Griffith, G.J. Lush, A.J. Metheringham and R.H. Thomas, Nucl. Phys. **60** (1964) 369-377.
[26] M.P. Nakada, J.D. Anderson, C.C. Gardner and C. Wong, Phys. Rev. **110** (1958) 1439.
[27] W. Bauhoff, Atomic Data and Nuclear Data Tables, **35** (1986) 429-447.
[28] A. Ingemarsson et al., Nucl. Phys. **A 676** (2000) 3.
[29] O.F. Nemets and L.I. Slyusarenko, Ser. Fiz. **54** (1990) 2105.
[30] L.V. Dubar, D.Sh. Eleukenov, L.I. Slyusarenko and N.P. Yurkuts, Yad. Fiz. **49** (1989) 1239 and Sov. J. Nucl. Phys. **49** (1989) 771.
[31] L.V. Dubar et al., Ser. Fiz. **50** (1986) 2034.
[32] G.P. Millburn, W. Birnbaum, W.E. Crandall and L. Schecter, Phys. Rev. **95** (1954) 1268.
[33] R.M. DeVries et al., Phys. Rev. C **26** (1982) 301.
[34] E. Labie, J. Lega, P. Leleux and P.C Macq, Nucl. Phys. **A 205** (1973) 81-89.
[35] A. Gökmen, H. Breuer, A.C. Mignerey, B.G. Glagola, K. Kwiatkowski and V.E. Viola, Jr., Phys. Rev. C **29** (1984) 1595.
[36] G. Igo and B.D. Wilkins, Phys. Rev. **131** (1963) 1251.
[37] N.S. Grigalashvili, N.K. Kutsidi, Yu.V. Teozadze and V.V. Topuridze, Yad. Fiz. **48** (1988) 476 and Sov. J. Nucl. Phys. **48** (1988) 301.
[38] E.O. Abdrakhmanov *et al.*, JINR, Dubna, preprint JINR El-11517. (1978).
[39] SKM-200 Collaboration: V.D. Aksinenko et al., Nucl. Phys. **A 348** (1980) 518.
[40] V.G. Ableyev *et al.*, JINR, Dubna, report JINR Pl-10565 (1977).
[41] L.N. Bokova *et al.*, JINR, Dubna, report JINR Pl-9364 (1975).
[42] I. Tanihata, Hyperfine Int. **21** (1985) 251.
[43] I. Tanihata et al., Phys. Rev. Lett. **55** (1985) 2676.
[44] W.R. Webber, J.C. Kish and D.A. Schrier, Phys. Rev. C **41** (1990) 520.
[45] C. A. Bertulani and C. De Conti, Phys. Rev. C **81** (2010) 064603
[46] J. Beringer et al. (Particle Data Group), Phys. Rev. D86, 010001 (2012) and 2013 partial update for the 2014 edition. http://pdg.lbl.gov/2013/hadronic-xsections/hadron.html http://pdg.lbl.gov/.
[47] L. Sihver, K. Aleklett, W. Loveland, P.L. McGaughey, D.H.E Gross and H.R. Jaqaman, Nucl. Phys. A 543, 703 (1992).
[48] K. Aleklett, W. Loveland and L. Sihver, Fizika 19, S71 (No. 1) (1987).
[49] K. Aleklett, L. Sihver and W. Loveland, Phys. Lett. B 197, 34 (1987).
[50] W. Loveland, M. Hellström, L. Sihver and K. Aleklett, Phys. Rev. C 42, 1753 (1990).
[51] R.D. Albert and L.F. Hansen, Phys. Rev. **123** (1961) 1749.
[52] K. Bearpark, W.R. Graham and G. Jones, Nucl. Phys. **73** (1965) 206.
[53] P.J. Bulman, G.W. Greenlees and M.J. Sametband, Nucl. Phys. **69** (1965) 536.
[54] R. Goloskie and K. Strauch, Nucl. Phys. **29** (1962) 474.
[55] T.J. Gooding, Nucl. Phys. **12** (1959) 241.
[56] A. Johansson, U. Svanberg and O. Sundberg, Arkiv Fysik **19** (1961) 527.
[57] A.J. Kirschbaum, PhD Thesis UCLA (1952), Technical report UCRL-1967.
[58] P. Kirkby and W.T. Link, Can. J. Phys. **44** (1966) 1847.
[59] K. Kwiatkowski, S.H. Zhou, T.E. Ward, V.E. Viola, Jr., H. Breuer, G.J. Mathews, A. Gökmen and A.C. Mignerey, Phys. Rev. Lett. **50** (1983) 1648.
[60] E. Labie, J. Lega, P. Leleux and P.C Macq, Nucl. Phys. **A 205** (1973) 81-89.

[61] M.Q. Makino, C.N. Waddell and R.M. Eisberg, Nucl. Phys. **50** (1964) 145.
[62] W.F. McGill, R.F. Carlson, T.H. Short, J.M. Cameron, J.R. Richardson, I. Slaus, W.T.H. van Oers, J.W. Verba, D.J. Margaziotis and P. Doherty, Phys. Rev. C **10** (1974) 2237.
[63] J.J.H. Menet, E.E. Gross, J.J. Malanify and Z. Zucker, Phys. Rev. C **4** (1971) 1114.
[64] V. Meyer, R.M. Eisberg and R.F. Carlson, Phys. Rev. **117** (1960) 1334.
[65] V. Meyer and N.M. Hintz, Phys. Rev. Lett. **5** (1960) 207.
[66] N. Okumura, Y. Aoki, T. Joh, Y. Honkyu, K. Hirota and K.S. Itoh, Nucl. Instrum. Meth. **A 487** (2002) 565.
[67] R.E. Pollock and G. Schrank, Phys. Rev. **140** (1965) B 575.
[68] B.D. Wilkins and G. Igo, Phys. Rev. **129** (1963) 2198.
[69] B.V. Zhuravlev, O.V. Grusha, S.P. Ivanova, V.I. Trykova and Y.N. Shubin, Yad. Fiz. **39** (1984) 264 and Sov. J. Nucl. Phys. **39** (1984) 164.
[70] R. Abegg et al., Nucl. Phys. **A 324** (1979) 109-114.
[71] R.D. Albert and L.F. Hansen, Phys. Rev. **123** (1961) 1749.
[72] K. Bearpark, W.R. Graham and G. Jones, Nucl. Phys. **73** (1965) 206.
[73] K. Bearpark, W.R. Graham and G. Jones, Nucl. Instrum. Meth. **35** (1965) 235.
[74] A.J. Elwyn, A. Marinov and J.P. Schiffer, Phys. Rev. **145** (1966) 957.
[75] M. Enke et al., Nucl. Phys. **A 657** (1999) 317.
[76] C. Hojvat and G. Jones, Nucl. Instrum. Meth. **66** (1968) 13.
[77] A. Johansson, U. Svanberg and O. Sundberg, Arkiv Fysik **19** (1961) 527.
[78] P.A. Gottschalk et al., Phys. Rev. Lett. **42** (1979) 359.
[79] V.V. Gachurin, B.L. Druzhinin, B.A. Ezhov et al., Technical report: Gosudarsivennyi Komitet po Ispol'zovaniyu Atomnol Energii SSSR, Moscow, Inst. Teoretie heskoi i Eksperimental'noi Fiziki, ITEF-59 (1985).
[80] B.M. Bobchenko et al., Yad. Fiz. **30** (1979) 1553 and Sov. J. Nucl. Phys. **30** (1979).
[81] A.J. Kirschbaum, PhD Thesis UCLA (1952), Technical report UCRL-1967.
[82] V.G. Ableev et al., Yad. Fiz. **42** (1985) 205 and Sov. J. Nucl. Phys. **42** (1985) 129.
[83] A. Ingemarsson et al., Nucl. Phys. **A 696** (2001) 3.
[84] V.N. Domnikov et al., Ser. Fiz. **52** (1988) 899.
[85] V.G. Ableyev *et al.*, JINR, Dubna, report JINR Pl-10565 (1977).
[86] A. Budzanowski et al., Nucl. Phys. **A 106** (1968) 21.
[87] V.P. Badovskii et al., Ser. Fiz. **51** (1987) 201.
[88] D. Shapira, J.L.C. Ford, Jr. and J. Gomez del Campo, Phys. Rev. C **26** (1982) 2470.
[89] D.Q. Fang et al., Eur. Phys J. **A 12** (2001) 335.
[90] H.Y. Zhang et al., Nucl. Phys. **A 707** (2002) 303.
[91] X.Z. Cai et al., Phys. Rev. C **65** (2002) 024610.
[92] L. Chulkov et al., Nucl. Phys. **A 603** (1996) 219.
[93] G.D. Westfall, LBL Report-7162 (1978).
[94] P. Ferrando, W.R. Webber, P. Goret, J.C. Kish, D.A. Schrier, A. Soutoul and O. Testard, Phys. Rev. C **37** (1988) 1490.
[95] G.D. Westfall, L.W. Wilson, P.J. Lindstrom, H.J. Crawford, D.E. Greiner and H.H. Heckman, Phys. Rev. C **19** (1979).
[96] A. Kohama, K. Iida, K. Oyamatsu, H. Iwase, and K. Niita, RIKEN Accelerator Progress Report Vol. **44** (2010) p. 47, http://www.nishina.riken.jp/researcher/APR/archive_e.html.

Figure labels

Figure 1. Calculated total reaction cross sections for $^{12}C + ^{12}C$ using the BS model (black solid line) and the Tripathi parameterization (black dashed line) are shown together with the calculated cross sections using the Hybrid Kurotama model (solid red line) and experimental data from [13-18].

Figure 2. Calculated total reaction cross sections using the Hybrid Kurotama model (solid red line), before the improvements of the model presented in this paper were implemented, are shown for for $p+^{4}He$ together with the calculated cross sections using the Tripathi parameterization (black dashed line) and experimental data from [18-27].

Figure 3. Calculated total reaction cross sections using the Hybrid Kurotama model (solid red line), before the improvements of the model presented in this paper were implemented, are shown for $^{4}He+^{12}C$ together with the calculated cross sections using the Tripathi parameterization (black dashed line) and experimental data from [18, 28-44].

Figure 4. Calculated total reaction cross sections using the improved Hybrid Kurotama model (solid red line) are shown for $p+^{4}He$ together with the calculated cross sections using the Tripathi parameterization (black dashed line) and experimental data from [18-27].

Figure 5. Calculated total reaction cross sections using the improved Hybrid Kurotama model (solid red line) are shown for $p+^{27}Al$ together with the calculated cross sections using the Tripathi parameterization (black dashed line) and experimental data from [32,51-69].

Figure 6. Calculated total reaction cross sections using the improved Hybrid Kurotama model (solid red line) are shown for $p+^{197}Au$ together with the calculated cross sections using the Tripathi parameterization (black dashed line) and experimental data from [54,70-77].

Figure 7. Calculated total reaction cross sections using the improved Hybrid Kurotama model (solid red line) are shown for p + U together with the calculated cross sections using the Tripathi parameterization (black dashed line) and experimental data from [32,52,78-81].

Figure 8. Calculated total reaction cross sections using the improved Hybrid Kurotama model(solid red line) are shown for $^{3}He+^{12}C/C$ together with the calculated cross sections using the Tripathi parameterization (black dashed line) and experimental data from [32,82,83].

Figure 9. Calculated total reaction cross sections using the improved Hybrid Kurotama model (solid red line) are shown for $^{4}He+^{54}Fe/^{56}Fe/Fe$ together with the calculated cross sections using the Tripathi parameterization (black dashed line) and experimental data from [18,28,29,31-33,35,36,82-83].

Figure 10. Calculated total reaction cross sections using the improved Hybrid Kurotama model (solid red line) are shown for $^{4}He+^{27}Al$ together with the calculated cross sections using the Tripathi parameterization (black dashed line) and experimental data from [31,36,39,84,85]

Figure 11. Calculated total reaction cross sections using the improved Hybrid Kurotama model (solid red line) are shown for $^{4}He+^{56}Fe$ together with the calculated cross sections using the Tripathi parameterization (black dashed line) and experimental data from [36,44,84-87]

Figure 12. Calculated total reaction cross sections using the improved Hybrid Kurotama model (solid red line) are shown for $^{12}C+^{12}C$ together with the calculated cross sections using the Tripathi parameterization (black dashed line) and experimental data from [13-18].

Figure 13. Calculated total reaction cross sections using the improved Hybrid Kurotama model (solid red line) are shown for $^{20}Ne+^{12}C$ together with the calculated cross sections using the Tripathi parameterization (black dashed line) and experimental data from [15,44, 88-95]. Please, notice that some of the experimental data are total charge changing cross sections.

Figure 14. Calculated total reaction cross sections using the improved Hybrid Kurotama model (solid red line) are shown for $^{12}C+^{54}Fe/^{56}Fe$ together with the calculated cross sections using the Tripathi parameterization (black dashed line) and experimental data from [14,15,44,93-95].

Figures

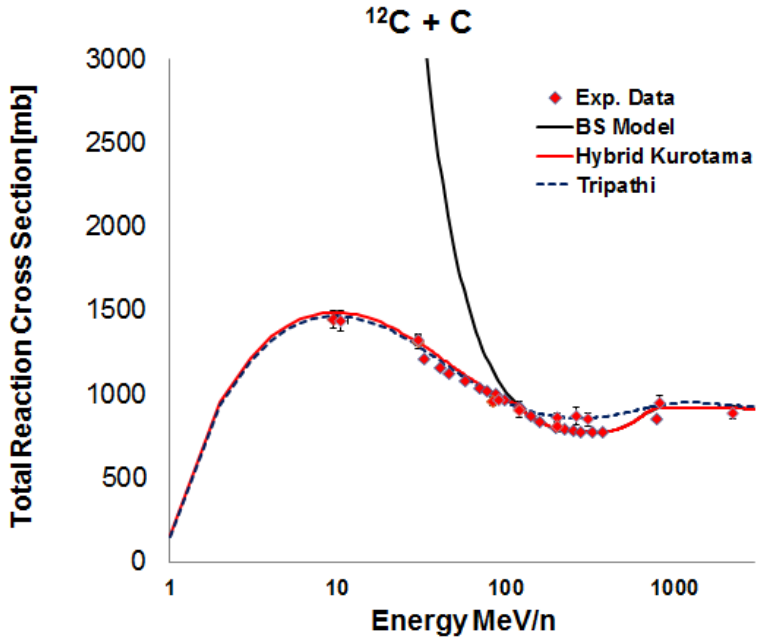

Figure. 1.

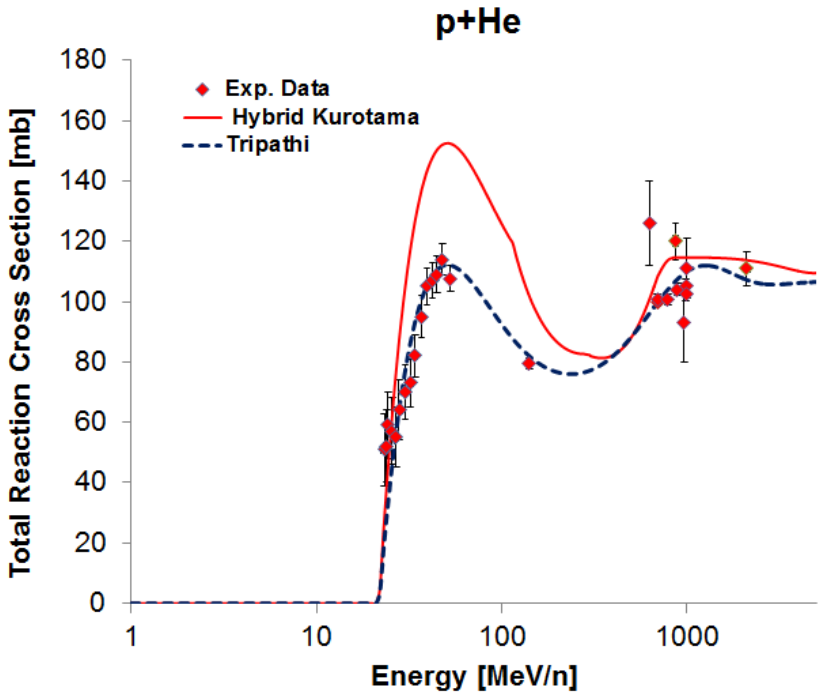

Figure. 2.

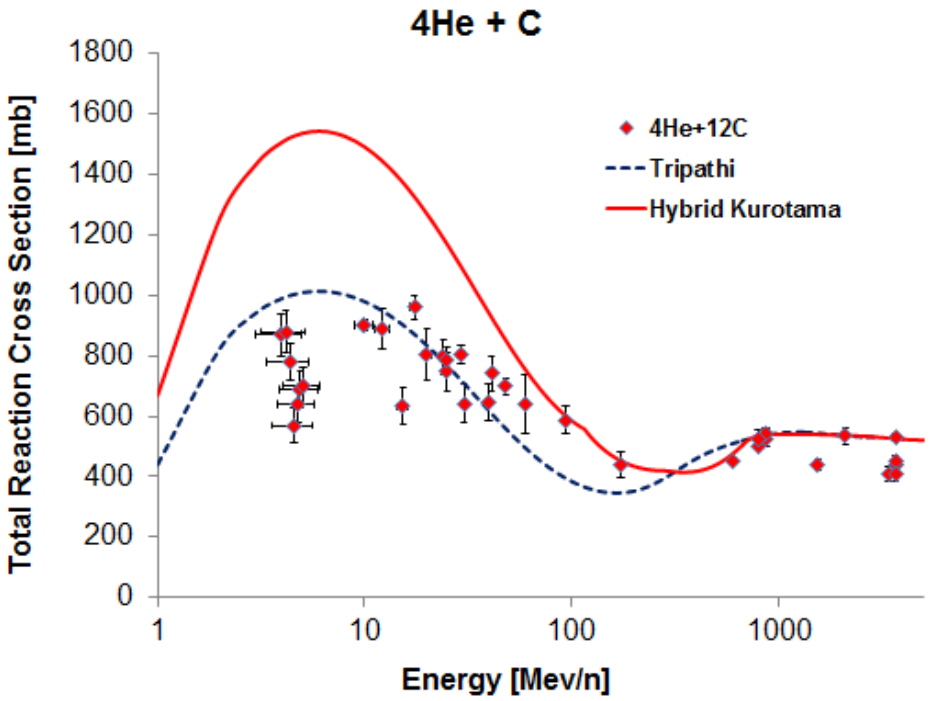

Figure. 3.

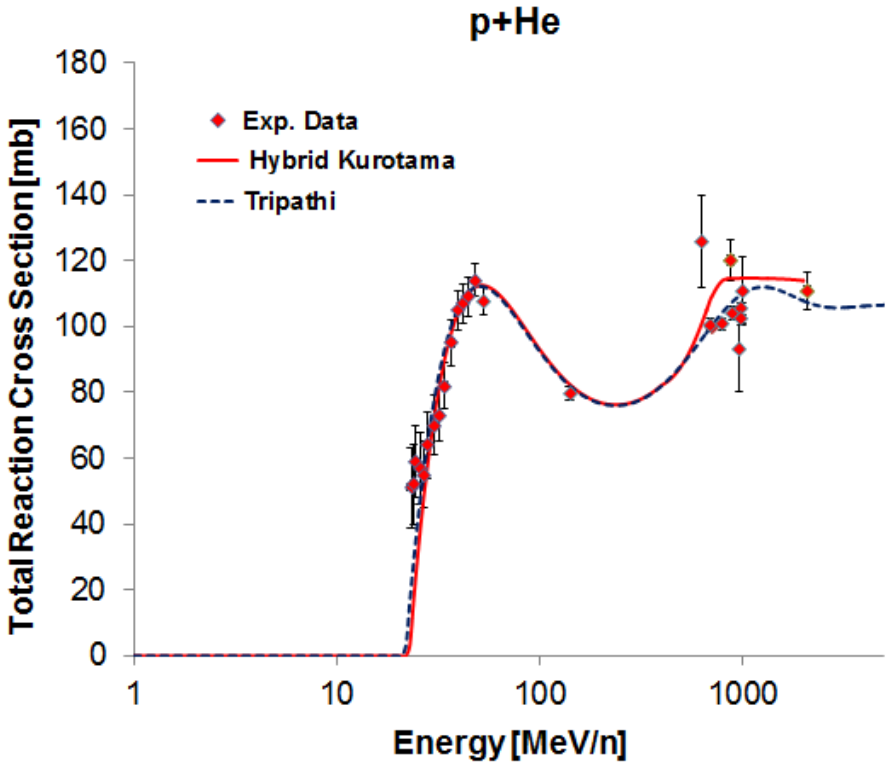

Figure. 4.

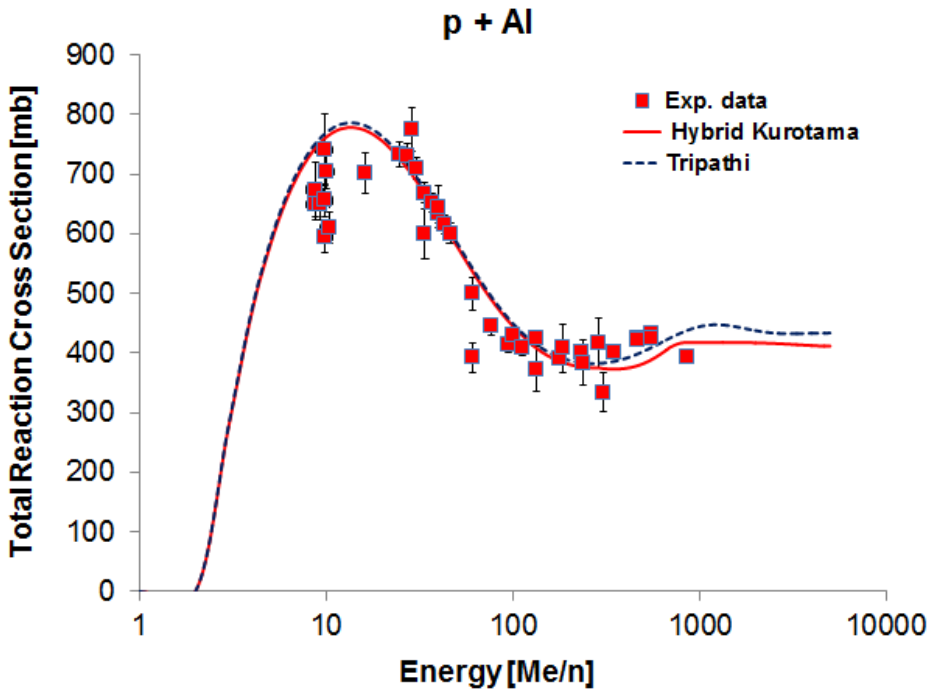

Figure. 5.

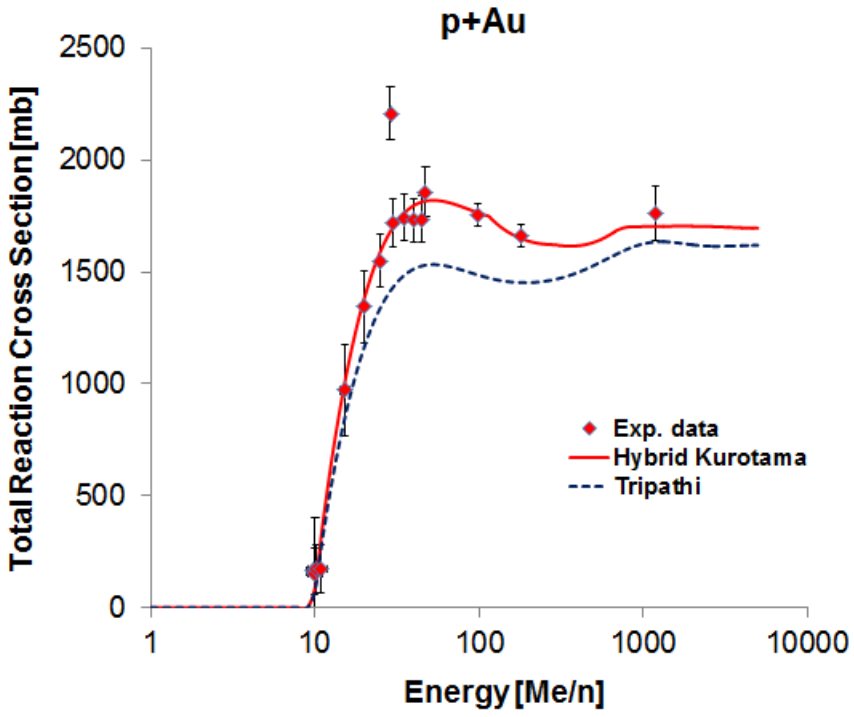

Figure. 6.

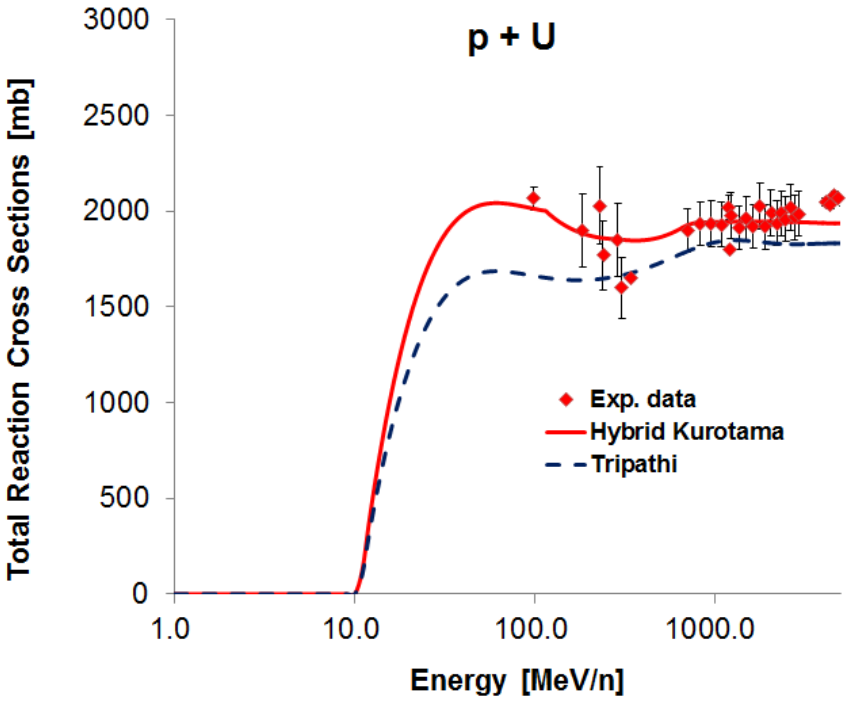

Figure. 7.

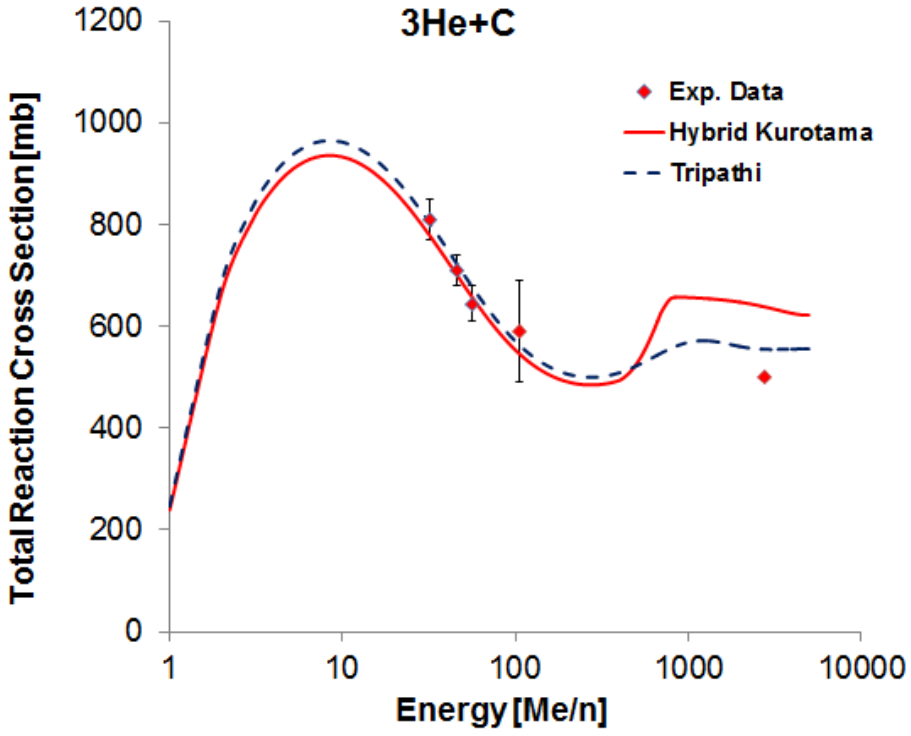

Figure. 8

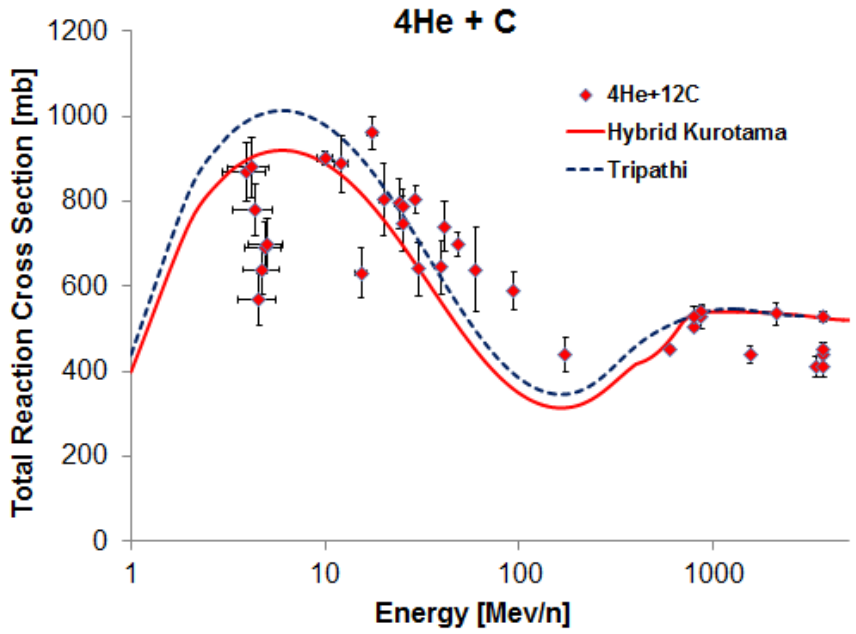

Figure.9.

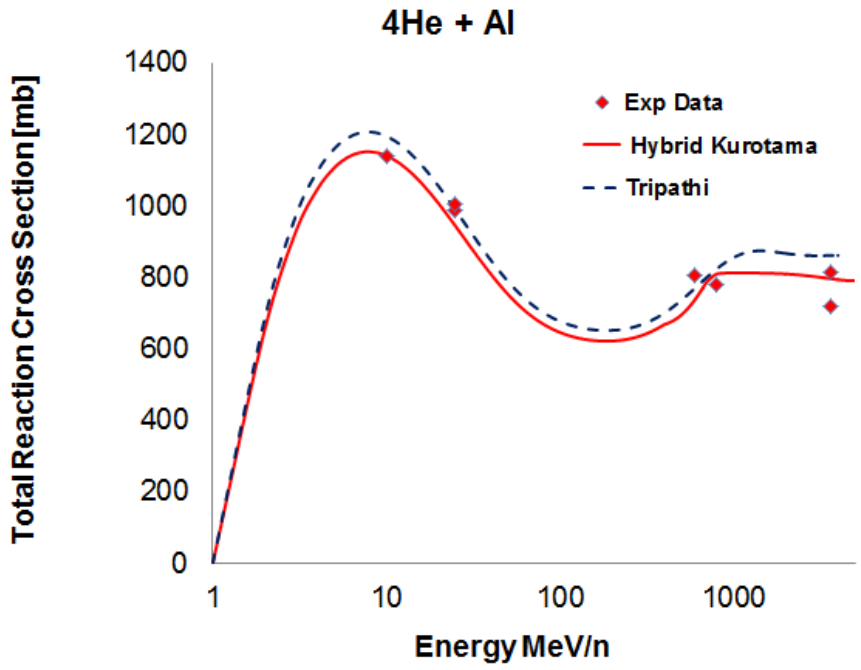

Figure. 10

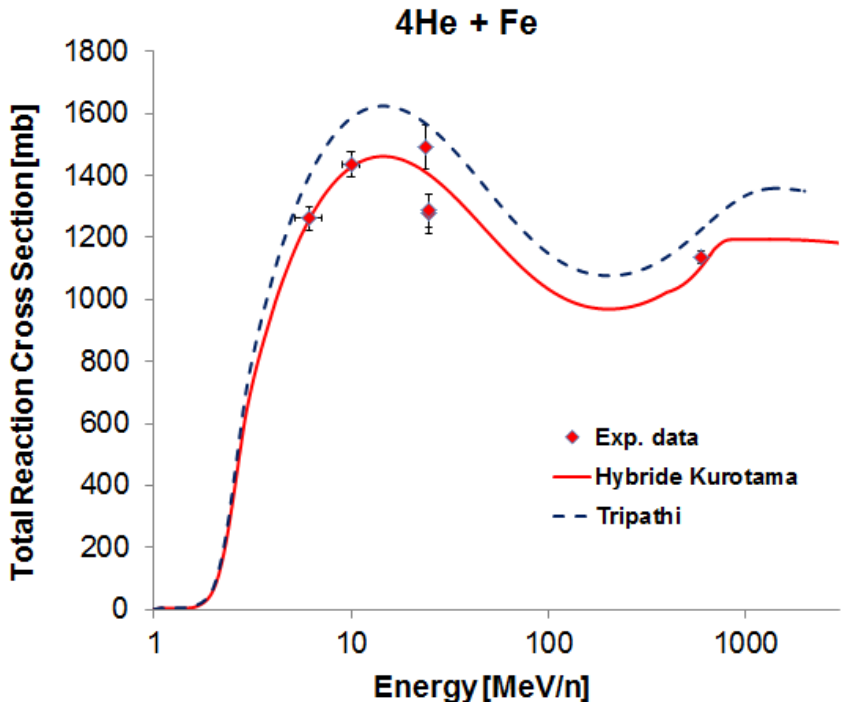

Figure. 11.

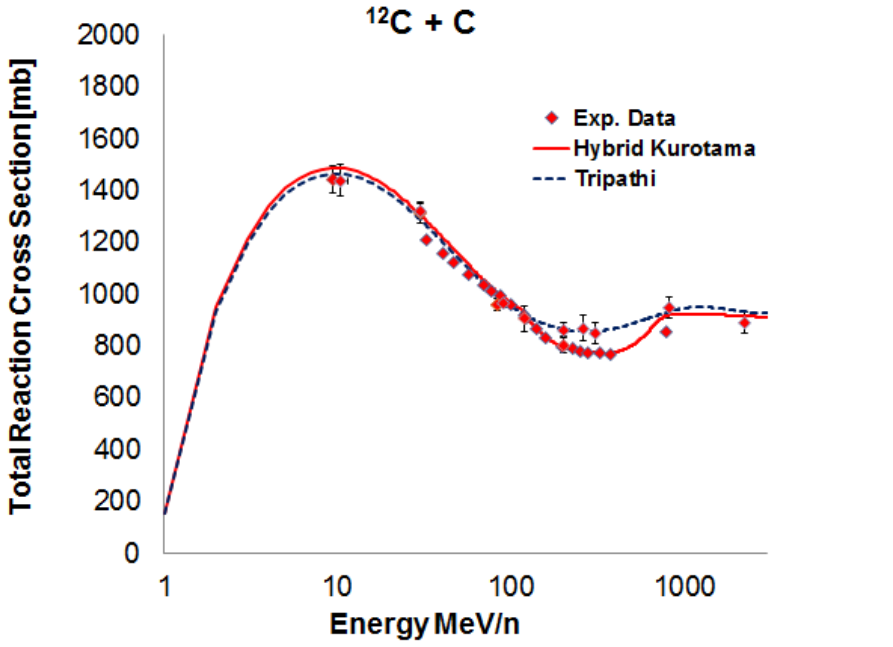

Figure. 12.

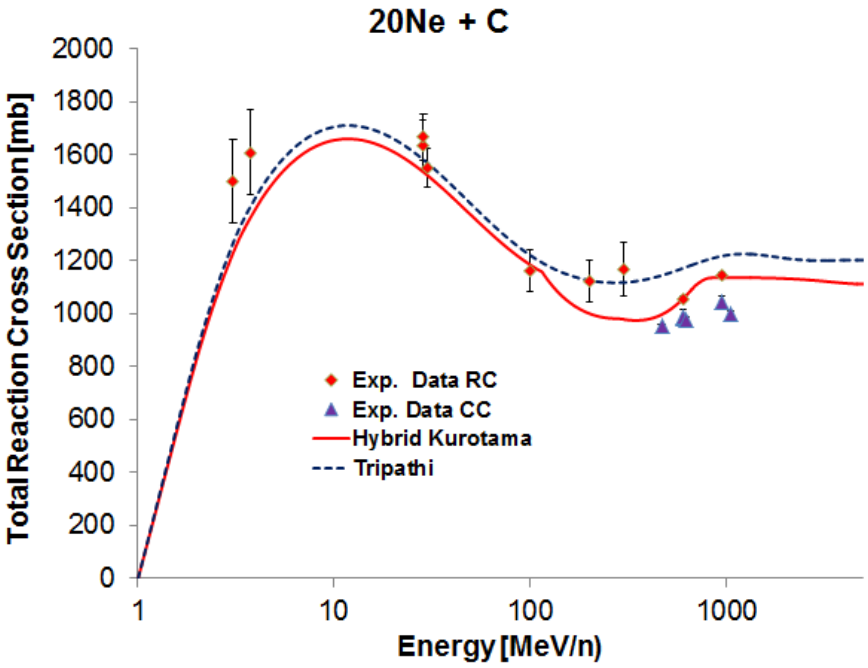

Figure. 13.

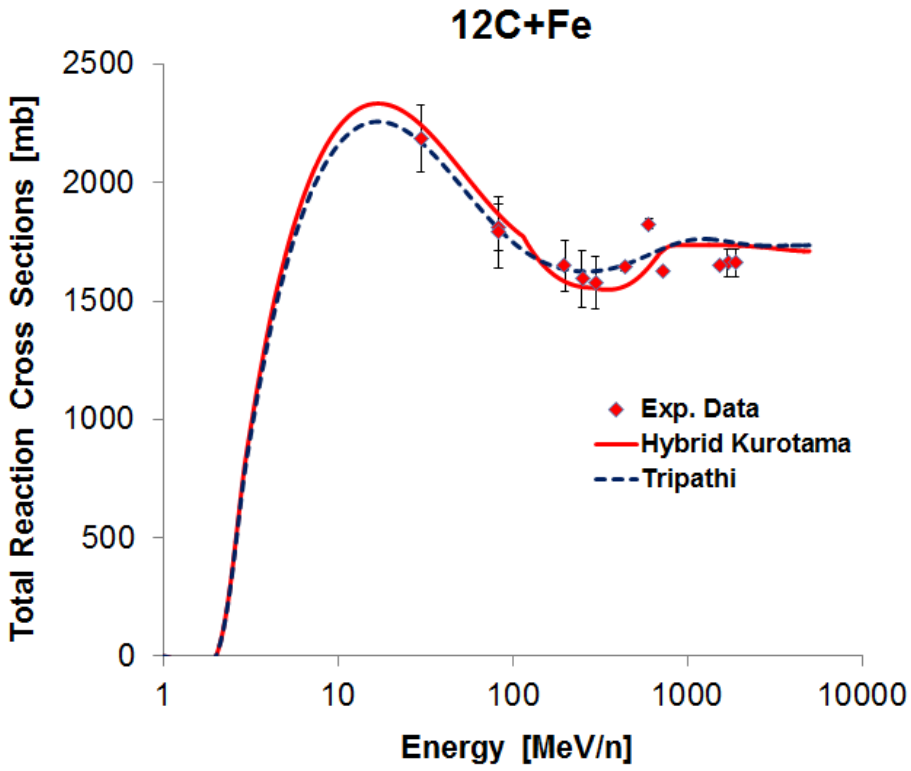

Figure. 14.